Available online at www.sciencedirect.com
SCIENCE DIRECT®
Physica B 368 (2005) 151–156
PHYSICA B
www.elsevier.com/locate/physb

Variation of group velocity and complete bandgaps in two-dimensional photonic crystals with drilling holes into the dielectric rods

Wen-Long Liu*, Tzong-Jer Yang

Department of Electrophysics, National Chiao Tung University, Hsinchu 30050, Taiwan, ROC

Received 22 June 2005; received in revised form 12 July 2005; accepted 12 July 2005

Abstract

Two-dimensional square lattices of square cross-section dielectric rods in air, designed with an air hole drilled into each square rod, are studied theoretically. By adjusting the shift of the hole position in the square rod in each unit cell, the dielectric distribution of the square rod will be modified. A sizable complete band gap occurs for certain structural parameters and exhibits very flat photonic bands near such gap edge, which resulting in a sharp peak of density of states. In addition, the zero or small group velocities are observed in a broad region of **k**-space. This structure can be fabricated with materials widely used today and opens a fascinating area for applications in optoelectric devices.
© 2005 Elsevier B.V. All rights reserved.

PACS: 42.70.Qs; 42.25.Bs; 41.20.−q

Keywords: Photonic band gap; Photonic crystals; Density of states; Group velocity

1. Introduction

First introduced by Yablonovitch [1] and John [2] in 1987, photonic crystals (PCs) are now a fascinating issue of research. PCs are of artificial materials having the periodical modulation of dielectric structures in space and there exist photonic band gaps (PBGs) in which the propagation of electromagnetic (EM) waves in any propagating direction and polarization state is inhibited. In the PBG the spontaneous emission from the atoms or molecules can be rigorously forbidden [1]. The absence of normal modes of EM waves along certain directions provides the potential for application to various optical devices, such as resonant antennas [3], microscopic lasers [4], and optical switches [5], etc.

The wider a PBG is, the greater the forbidden region of the frequency spectrum. Thus, the search for photonic crystals that possess wider band gaps

*Corresponding author. Tel.: +886 3 5720635; fax: +886 3 5725230.
E-mail address: wlliuz@ms48.hinet.net (W.-L. Liu).

0921-4526/$ - see front matter © 2005 Elsevier B.V. All rights reserved.
doi:10.1016/j.physb.2005.07.010

is an important issue. Various methods for creating large PBGs or in increasing an existing PBG by altering the dielectric constant $\varepsilon(\mathbf{r})$ within a unit cell, have been proposed. These methods include rotating the lattices [6], using anisotropic dielectric materials [7], rotating the noncircular rods [8–10], and modifying the permittivity distribution in a unit cell [11–13]. In such cases, an EM wave can be decomposed into the *E*- and *H*-polarization modes for two-dimensional (2D) photonic crystal. A complete PBG exists for 2D PBG crystal only when band gaps in both *E*- and *H*-polarization modes are present and they overlap each other. That is a PBG independent of the polarization of the EM waves. Many crystals generating band gaps for some light polarizations, but these may not overlap to produce a complete PBG [14]. It was reported that the symmetry reduction of atom configuration by introducing a two-point basis set in simple 2D lattice can remarkably increase complete PBG [15], quite similar to the 3D case for diamond structure [16]. In contrast, symmetry breaking in a square lattice by changing the shape of square air rods to rectangular [17] or cylinder [18] reduces the width of complete PBGs.

In this work we study a type of square photonic lattice in two dimensions, which is formed by an air hole drilled into each square dielectric rod in air. We shift the air hole to modify dielectric distribution without changing the shape and orientation of dielectric scatterers. A sizable complete PBG occurs for certain structural parameters and exhibits very flat photonic bands near such gap edge, which results in a sharp peak of density of states. In addition, the zero or small group velocities are observed in a broad region of **k**-space. These small group velocities of the eigenmode cause a long optical path in this structure [19]. It brings about the optical gain enhancement or low-threshold lasing [20,21].

2. Theory

Fig. 1 displays the schematic diagram of our proposed 2D photonic band structure. The square dielectric rods with a side-length of l and dielectric

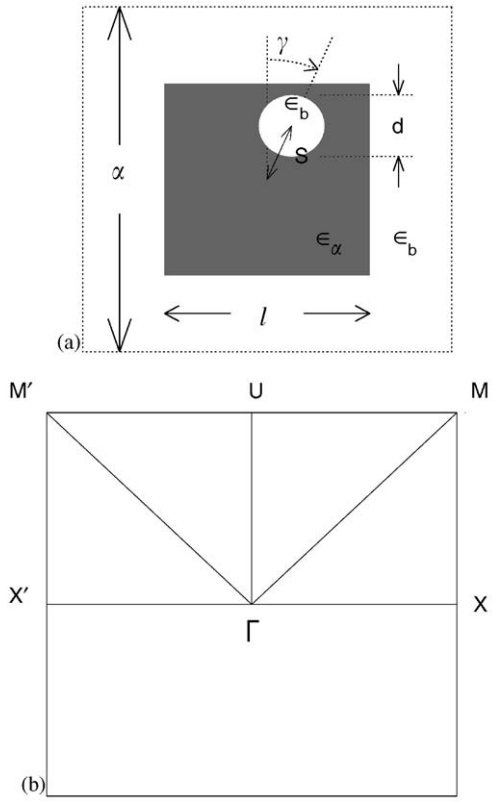

Fig. 1. (a) Schematic diagram of proposed photonic crystals. The square dielectric rods with a side-length of l and dielectric ε_a are placed in air background with $\varepsilon_b = 1.0$ at the center of a 2D square lattice with a lattice constant, a, in the xy-plane. Another circular rod with $\varepsilon_b = 1.0$ and diameter d is drilled into square rod in each unit cell. We denote $\beta = d/l$ for convenience. We assume that there is a shift **s** of the drilled circular rod with respect to the center of the unit cell, that is $\mathbf{s} = s(\hat{\mathbf{x}}\sin\gamma + \hat{\mathbf{y}}\cos\gamma)$, where γ is the span angle of the displacement vector with respect to the y-axis, (b) the Brillouin zone with symmetry points, **Γ**, **X**, **M**, **U**, **M**′ and **X**′.

ε_a are placed in air background with $\varepsilon_b = 1.0$ at the center of a 2D square lattice with a lattice constant, a, in the xy-plane. Another circular rod with $\varepsilon_b = 1.0$ and diameter d is drilled into square rod in each unit cell. We denote $\beta = d/l$ for convenience.

The electromagnetic (EM) fields with the E/H-polarization (in-pane magnetic/electric fields) in the 2D PC are governed by Maxwell's equations:

$$\left\{\nabla \times \frac{1}{\varepsilon(\mathbf{r})}\nabla\times\right\}\mathbf{H}(\mathbf{r}) = \frac{\omega^2}{c^2}\mathbf{H}(\mathbf{r}), \tag{1}$$

where $\mathbf{H}(\mathbf{r})$ denotes the magnetic fields; ω the angular frequency; c the speed of light in vacuum, and $\varepsilon(\mathbf{r})$ the periodically modulated dielectric function. The magnetic fields and the dielectric function can be expanded in terms of Fourier series as

$$\mathbf{H}(\mathbf{r}) = \sum_{\mathbf{G}} \sum_{\lambda=1}^{2} h_{\mathbf{G},\lambda} \hat{\mathbf{e}}_{\lambda} e^{i(\mathbf{k}+\mathbf{G})\cdot\mathbf{r}}, \tag{2}$$

$$\varepsilon(\mathbf{r}) = \sum_{\mathbf{G}} \varepsilon(\mathbf{G}) e^{i\mathbf{G}\cdot\mathbf{r}}, \tag{3}$$

where $\mathbf{k}$ is the Bloch wave vector within the first Brillouin zone, and $\mathbf{G}$ the 2D reciprocal lattice vector. The polarization unit vectors $\hat{\mathbf{e}}_{\lambda}$ with $\lambda = 1, 2$ are perpendicular to $(\mathbf{k}+\mathbf{G})$, and $h_{\mathbf{G},\lambda}$ is the Fourier expansion component of the magnetic fields.

The Fourier coefficient $\varepsilon(\mathbf{G})$ is given by

$$\varepsilon(\mathbf{G}) = \frac{1}{A_{\text{cell}}} \int_{\text{cell}} \varepsilon(\mathbf{r}) e^{-i\mathbf{G}\cdot\mathbf{r}} \, d\mathbf{r}, \tag{4}$$

where the integration is performed over the unit cell. Here, the filling factor f, which is the ratio of the areas A_{scat} of dielectric scatterers in a unit cell to the area A_{cell} of a unit cell of square lattice, is

$$f = \frac{l^2}{a^2}\left(1 - \frac{\pi\beta^2}{4}\right). \tag{5}$$

For the proposed PC, $\varepsilon(\mathbf{G})$ is evaluated by

$$\varepsilon(\mathbf{G}) = \begin{cases} f\varepsilon_a + (1-f)\varepsilon_b & \text{for } \mathbf{G} = 0, \\ (\varepsilon_a - \varepsilon_b) S(\mathbf{G}) & \text{for } \mathbf{G} \neq 0. \end{cases} \tag{6}$$

We assume that there is a shift $\mathbf{s}$ of the drilled circular rod with respect to the center of the unit cell, that is $\mathbf{s} = s(\hat{\mathbf{x}}\sin\gamma + \hat{\mathbf{y}}\cos\gamma)$, where γ is the span angle of the displacement vector with respect to the y-axis. The structural factor $S(\mathbf{G})$ is then given by

$$S(\mathbf{G}) = S_1(\mathbf{G}) - e^{-i\mathbf{G}\cdot\mathbf{s}} S_2(\mathbf{G}), \tag{7}$$

where

$$S_1(\mathbf{G}) = \left(\frac{l^2}{a^2}\right) \text{Sinc}\left(\frac{G_x l}{2}\right) \text{Sinc}\left(\frac{G_y l}{2}\right) \tag{8}$$

with $\text{Sinc}(x) = \sin x / x$ and

$$S_2(\mathbf{G}) = \left(\frac{l^2}{a^2}\right) \frac{\pi\beta^2}{2} \frac{J_1(Ga)}{Ga}, \tag{9}$$

where $J_1(x)$ is the Bessel function of the first kind, and $G = |\mathbf{G}|$.

The band structures are then determined from solving the following equation:

$$\sum_{\mathbf{G}'} A(\mathbf{k}+\mathbf{G}, \mathbf{k}+\mathbf{G}') H(\mathbf{G}') = \omega^2 H(\mathbf{G}) \tag{10}$$

with

$$A(\mathbf{K}, \mathbf{K}') = \begin{cases} |\mathbf{K}||\mathbf{K}'|\varepsilon^{-1}(\mathbf{K}-\mathbf{K}') & \text{for the } E\text{-polarization state,} \\ \mathbf{K}\cdot\mathbf{K}'\varepsilon^{-1}(\mathbf{K}-\mathbf{K}') & \text{for the } H\text{-polarization state,} \end{cases} \tag{11}$$

where $\mathbf{K} = \mathbf{k}+\mathbf{G}$, $\mathbf{K}' = \mathbf{k}+\mathbf{G}'$. $\varepsilon^{-1}(\mathbf{K}-\mathbf{K}') = \varepsilon^{-1}(\mathbf{G}-\mathbf{G}')$ can be computed from solving the following equation:

$$\sum_{\mathbf{G}''} \varepsilon^{-1}(\mathbf{G}-\mathbf{G}'')\varepsilon(\mathbf{G}''-\mathbf{G}') = \delta_{\mathbf{G}\mathbf{G}'}. \tag{12}$$

3. Results and discussion

All our calculations have been performed for $\varepsilon_a = \varepsilon = 13.6$ appropriate for gallium arsenide (GaAs), and $\varepsilon_b = 1.0$ in air. GaAs has been used because this material exhibits fascinating optical properties in the infrared region and is representative of many semiconductors. The design of this structure has many degrees of freedom which can be used to optimize the size of the gap, depending on the materials used in the fabrication. Although GaAs is used in this example, they can be replaced by other material with a different index contrast. To calculate PBGs for the $E(H)$-polarization 1521 plane waves in the Fourier expansion are used. First, the PBG structures and the corresponding density of states (DOS) of an air hole drilled into the center of each square dielectric rod in each unit cell are calculated, as shown in Fig. 2(a). The parameters in this figure are chosen as $a/l = 1.63$, $\beta = 0.35$ (corresponding to filling factor $f = 0.34017$) and $s = 0$. The solid (dotted)

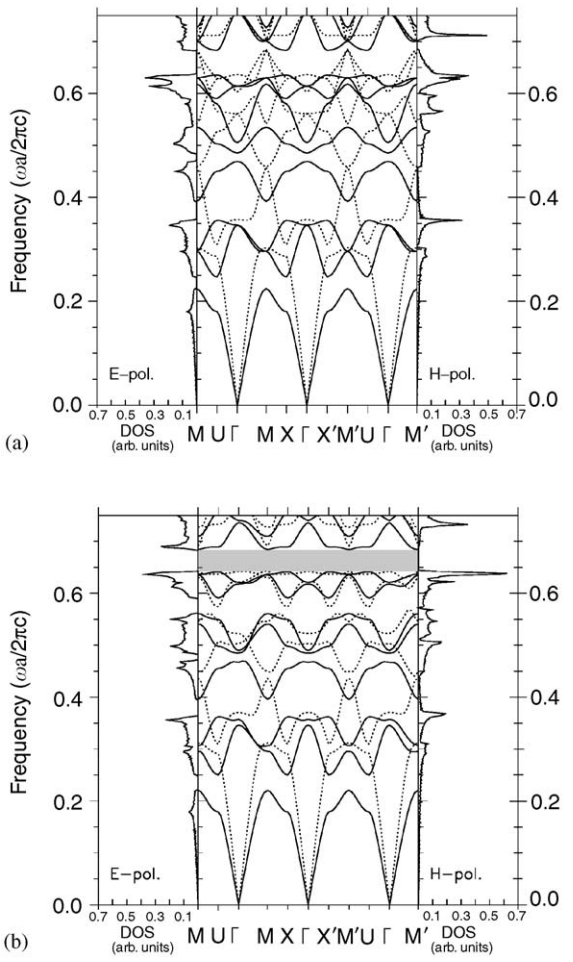

Fig. 2. Photonic band structures and the corresponding density of states (DOS) for two structures. The parameters in this figure are chosen as $a/l = 1.63$, $\beta = 0.35$ (corresponding to filling factor $f = 0.34017$). (a) $s = 0$ and (b) $s = 0.11$, $\gamma = 45^\circ$. The solid and dotted curves correspond to the E- and H-polarizations, respectively. The shadow area marks the complete gap region.

curves correspond to the $E(H)$-polarization. It is shown that there are four PBGs for the E-polarization and two PBGs for the H-polarization. However, overlap of PBG for E- and H-polarization does not exist. Along the left-hand and right-hand margins of this figure the density of photonic states in arbitrary units were plotted. The eigenfrequencies for 6400 uniformly spaced values of **k** vectors inside the first Brillouin zone were calculated. In Fig. 2(b), the calculated result for $s = 0.11a$ and $\gamma = 45^\circ$ is illustrated. The other parameters are the same as those quoted in Fig. 2(a). A complete PBG with a gapwidth of $\Delta\omega = 0.0415(2\pi c/a)$, and a central value, $\omega_g = 0.66335(2\pi c/a)$, which is in the region of overlap of E_8 and H_6 band gaps, is found. E_i and H_i denotes the gaps that appear between the ith and $(i+1)$th bands, for the corresponding polarization. In the spectral range of this complete bandgap neither E-polarized nor H-polarized photonic states exist (DOS = 0). Notably, modifying the position of circular hole in the square dielectric rod in air seems to lower the frequency of the ninth E-polarization band and the fifth and sixth H-polarization bands at the $\mathbf{M}(\mathbf{M}')$ point of the Brillouin zone that depicted in Fig. 2(a), then the overlap of E_8 and H_6 band gaps occurs. This result can be understood to be due to the fact that reducing the symmetry of the dielectric distribution in the square rod. Apparently, the band structure in Fig. 2(b) also exhibits very gently sloped bands near the complete PBGs edge. Thus, a sharp peak of density of states can be observed due to the flat band. Since the group velocity v_g of the modes given by the slope of the dispersion curves, $\partial\omega/\partial k$, is expected to be zero or very small and correspondingly, the optical path is expected to be long. Comparison between Fig. 2(a) and (b) shows that the zero or small group velocities are observed in a broad region of **k**-space as the increase of **s**. The fifth, sixth H-polarization bands and the ninth E-polarization band become more restricted to a narrow spectral region, thus, light waves become more localized as **s** increased. There are **k** points between the M–U direction at which the sixth H-polarization and the eighth E-polarization bands are almost flat. That is to say, group velocities of both mode approach to zero. Generally, the zero group velocity appears near photonic band edge only for E- or H-polarization. In this case, the zero group velocity is allowed for both E- and H-polarization simultaneously.

An additional plot in Fig. 3 provides more information on PCs. The PBG map as the relative shift s of the drilled rod for three different directions of (a) $\gamma = 0^\circ$, (b) $\gamma = 22.5^\circ$ and (c)

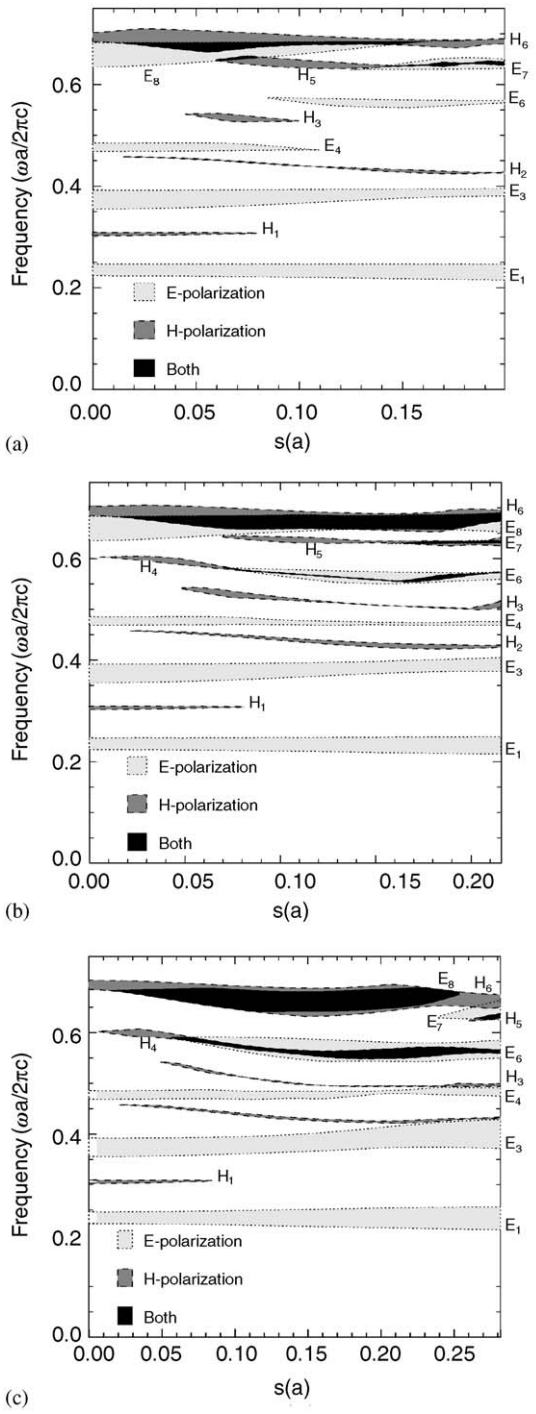

Fig. 3. The PBG map as the relative shift s of the drilled rod for three different directions of (a) $\gamma = 0^\circ$, (b) $\gamma = 22.5^\circ$ and (c) $\gamma = 45^\circ$. The other parameters are as those quoted in Fig. 2(a). The black area denotes the complete band gaps.

$\gamma = 45^\circ$. The other parameters are as those in Fig. 2(a). Only the first ten-bands are involved in this map for both E- and H-polarizations. Notably, for a given γ, the varying region of s is limited, i.e., only from zero to a certain value at which the outermost edge of the internal air circular rod just touches the outermost edge of the square dielectric rod at the lattice. The gap map for E-polarization shown in Fig. 3(a) exhibits six large gaps. We note that E_1 and E_3 gaps occur over the range of the shift s within $[0, 0.199]a$. Moreover, a remarkable gap H_6 occurs in the same range for H-polarization. Some other gaps only lie in the intermediate range of s. There are three complete PBGs in this configuration due to the overlap of E_8 with H_5; E_7 with H_5, and E_8 with H_6 gaps. Comparison among Fig. 3(a)–(c) shows that gap widths strongly depend on the shift of the air hole position. The most important result is the appearance of the overlap of E_8 with H_6 gap, which occurs for s in the region $[0.015, 0.18]a$ for $\gamma = 0^\circ$, $[0.016, 0.215]a$ for $\gamma = 22.5^\circ$ and $[0.014, 0.253]a$ for $\gamma = 45^\circ$, in turn. One would see this complete PBG to get larger width as the γ is increased. This complete PBG is always bounded at the top by the upper boundary of the E_8 gap. The lower boundary switches from H_6 to E_8 gap both in Fig. 3(a) and (b). Furthermore, its bottom side shown in Fig. 3(c) is wholly bounded by the lower boundary of the E_8 gap. In fact, since E and H polarized modes are decoupled and are governed by different equations for a right choice of s and γ.

We have also examined the case of an air hole drilled at the center of each square dielectric rod in air. Fig. 4 shows the PBG map as a function of the parameter β for filling factor $f = 0.34017$. Several gaps in both E- and H-polarization appear and disappear as β is varied. We should note here that one H-polarization and four E-polarization gaps exhibit near $\beta = 0$ when air hole is absent. One large complete PBG occurs due to the overlap of H_6 and E_8 gaps. This complete PBG starts near $\beta = 0$ and ends at about 0.34. The gap size $\Delta\omega$ reaches the maximum value $0.0427(2\pi c/a)$ at about $\beta = 0.19$ when the same total filling factor $f = 0.34017$ and $a/l = 1.69$.

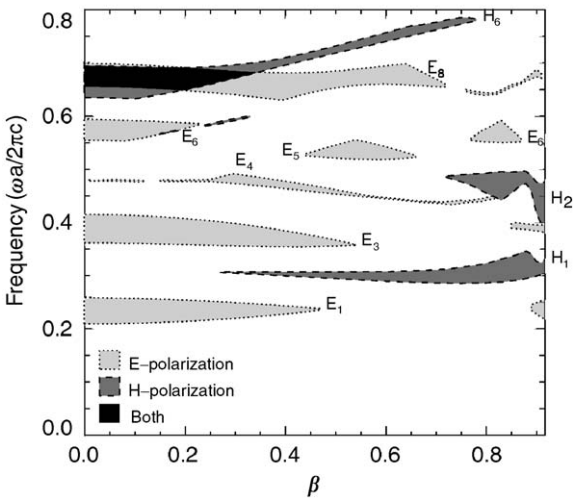

Fig. 4. The PBG map as a function of the parameter β for filling factor $f = 0.34017$, $s = 0$.

4. Conclusion

This study proposes two-dimensional square lattices of square cross-section dielectric rods in air, designed with an air hole drilled into each square rod. By adjusting the shift of the hole position in the square rod in each unit cell, the dielectric distribution of the square rod will be modified. The calculations show that the photonic crystal structure proposed here has a sizable complete band gap and exhibits very gently sloped bands near such gap edge, which resulting in a sharp peak of density of state. In addition, the zero or small group velocities are observed in a broad region of **k**-space. This property can be utilized for optical gain enhancement or low-threshold lasing.

Acknowledgements

The authors would like to thank the National Science Council of the Republic of China, Taiwan (Contract no. NSC 93-2112-M-009-010) and the Electrophysics Department, National Chiao Tung University, Taiwan, for their support. We acknowledge Ben-Yuan Gu for discussions.

References

[1] E. Yablonovitch, Phys. Rev. Lett. 58 (1987) 2059.
[2] S. John, Phys. Rev. Lett. 58 (1987) 2486.
[3] B. Temelkuran, M. Bayindir, E. Ozbay, R. Biswas, M.M. Sigalas, G. Tuttle, K.M. Ho, J. Appl. Phys. 87 (2000) 603.
[4] O. Painter, R.K. Lee, A. Scherer, A. Yariv, J.D. O'Brien, P.D. Dapkus, I. Kim, Science 284 (1999) 1819.
[5] K. Busch, S. John, Phys. Rev. Lett. 83 (1999) 967.
[6] C.M. Anderson, K.P. Giapis, Phys. Rev. B 56 (1997) 7313.
[7] Z.Y. Li, B.Y. Gu, G.Z. Yang, Phys. Rev. Lett. 81 (1998) 2574;
Z.Y. Li, B.Y. Gu, G.Z. Yang, Eur. Phys. J. B 11 (1999) 65.
[8] X.H. Wang, B.Y. Gu, Z.Y. Li, G.Z. Yang, Phys. Rev. B 60 (1999) 11417.
[9] C. Goffaux, J.P. Vigneron, Phys. Rev. B 64 (2001) 075118.
[10] N. Susa, J. Appl. Phys. 91 (2002) 3501.
[11] R.D. Meade, A.M. Rappe, K.D. Brommer, J.D. Joannopoulos, J. Opt. Soc. Am. B 10 (1993) 328.
[12] M. Qiu, S. He, J. Opt. Soc. Am. B 17 (2000) 1027.
[13] X.D. Zhang, Z.Q. Zhang, L.M. Li, C. Jin, D. Zhang, B. Man, B. Cheng, Phys. Rev. B 61 (2000) 1892.
[14] Z. Sun, T. Stirner, Physica B 322 (2002) 323.
[15] C.M. Anderson, K.P. Giapis, Phys. Rev. Lett. 77 (1996) 2949.
[16] K.M. Ho, C.T. Chan, C.M. Soukoulis, Phys. Rev. Lett. 65 (1990) 3152.
[17] P.R. Villeneuve, M. Piché, Phys. Rev. B 46 (1992) 4696.
[18] N. Susa, J. Appl. Phys. 91 (2002) 3501.
[19] J.P. Dowling, M. Scalora, M.J. Bloemer, C.M. Bowden, J. Appl. Phys. 75 (1994) 1896.
[20] S. Nojima, Japan J. Appl. Phys. 37 (2) (1998) L565.
[21] K. Sakoda, K. Ohtaka, T. Ueta 4 (1999) 481.